Fabrication of Hydrogen-Selective Silica Membranes via Pyrolysis of Vapor Deposited Polymer Films

Bryan Nguyen, Sasan Dabir, Theodore Tsotsis, Malancha Gupta*

Mork Family Department of Chemical Engineering and Materials Science, University of Southern California, 925 Bloom Walk, Los Angeles, California 90089, United States

*Corresponding Author Email: malanchg@usc.edu

Keywords: Membranes, Chemical Vapor Deposition, Silica

Abstract

Efficient separation of hydrogen under steam reforming conditions is important for the development of clean energy sources. Although high-temperature and steam-stable membranes with high fluxes and large separation factors would be valuable for such an application, their fabrication remains a challenge. Silicon-based ceramic membranes are particularly promising due to their high temperature resistance and excellent chemical stability. In this study, we propose a new synthetic route for fabricating nanoporous, asymmetric membranes via the pyrolysis of silicon-containing polymer films deposited by initiated chemical vapor deposition (iCVD) on macroporous silicon carbide supports. Specifically, we systematically investigated the change in the chemical structure of poly(2,4,6,8-tetravinyl-2,4,6,8-tetramethyl cyclotetrasiloxane) films at different pyrolysis temperatures and found that the complete transition to a silica membrane occurred at ~1100 °C. Three different supports composed of silicon carbide powders of varying sizes were tested for membrane preparation. It was found that membranes formed with our process were microporous with separation factors several times above the corresponding Knudsen factors. Our synthetic route, therefore, offers a scalable and solventless method for producing silicon-based ceramic membranes for high-temperature separation and sensor applications.

Introduction

As the global energy demand continues to rapidly grow, hydrogen has been increasingly discussed as a viable alternative energy source for applications such as in hydrogen fuel cells. Approximately 50% of commercial hydrogen is currently produced via steam methane reforming (SMR), where methane reacts with high-pressure steam to form hydrogen and carbon monoxide, and the hydrogen is then extracted using adsorption[1] or membrane separation.[2,3] In order to reduce the cost of hydrogen for practical applications, it is important to optimize its production through SMR.[2,4] This highly endothermic reaction requires a large input of energy, with process temperatures as high as 850 °C typically employed.[5,6] In order to improve the efficiency of the reaction, membrane reactors have been studied as a promising alternative to the more conventional packed-bed reactor processes.[7]

One challenge in using such reactors is that the membranes, in addition to having good hydrogen permselectivity, must also be able to function in these extreme environments.[4–6] Inorganic membranes have several inherent advantages over their polymeric counterparts due to their superior chemical, thermal, and structural stability.[7–9] Current materials used as membranes for hydrogen separation include palladium,[9–11] zeolites,[4,9,12] and carbon molecular sieves.[13–15] Palladium and palladium-alloy membranes are currently the most commonly employed in SMR membrane reactor studies. However, these membranes are expensive and are susceptible to coking and hydrogen embrittlement which impart weaker thermal and mechanical properties causing the membranes to develop cracks under stress.[4,16] In addition, poisoning from sulfur-containing compounds negatively impacts separation performance. Zeolite membranes, while made of common materials, can have poor hydrogen selectivity under SMR conditions due to the presence of intercrystalline voids and they also lack long-term stability in the presence of steam and sulfur-

containing compounds.[4,9] Carbon-based membranes are highly selective toward hydrogen[4], and we are presently field-testing them in power generation applications.[13] However, these membranes have an upper temperature limit of operation of ~325 ºC and therefore they cannot be used in the SMR process which employs significantly higher temperatures.

Silicon-based membranes, such as those with chemical structures ranging from amorphous silica to pure SiC, have been shown to possess excellent hydrogen separation properties and do not have issues with hydrogen embrittlement and sulfur poisoning.[4,8,17] Current methods for producing these ceramic membrane films include solution-based techniques such as spin-coating[18] and dip-coating[19–21]. However, films fabricated with these solution-based methods have disadvantages such as substrate compatibility issues and difficulties with disposal of solvents.[22] Silicon-based membranes have also been produced using chemical vapor deposition (CVD)[17,23,24] and plasma-enhanced chemical vapor deposition (PECVD)[25,26] techniques. These deposition techniques often require high energy inputs that can damage the chemical functionality of the precursors, which hinders the ability to control the structure of the final ceramic produced.[22] In addition, PECVD reactors often employ processing conditions that induce a competition between deposition and etching of the film, which presents a challenge for controlling the thickness of the deposited coating.[22]

In this study, we introduce a new synthetic method to create robust asymmetric, nanoporous silica-based membranes using initiated chemical vapor deposition (iCVD) and subsequent pyrolysis. The iCVD process is an one-step, solventless process that utilizes a thermally-cleavable compound, such as tert-butyl peroxide, to initiate a free radical polymerization process.[22,27] Compared to other CVD processes, the iCVD process requires very low energy and mild reactor conditions and can employ a broad range of monomers to generate a variety of

polymer films.[22] It can be used to produce thin, conformal films over a wide variety of planar,[28] curved,[29] and porous surfaces.[30] In addition, the iCVD process can be scaled-up for roll-to-roll operation.[31] In this paper, we deposited poly(2,4,6,8-tetravinyl-2,4,6,8-tetramethyl cyclotetrasiloxane) (PV4D4) on a variety of silicon carbide supports fabricated from powders of various sizes. The pyrolysis of silicon-based polymers has been shown previously to form a variety of ceramics, ranging from silica to silicon oxycarbide and silicon carbide, for use in different applications including membranes.[32–36]

The macroporous support used during membrane preparation needs to be mechanically strong to withstand the high temperatures typically utilized in SMR and the high transmembrane pressure gradients imposed across during membrane reactor operation; it must also be resistant to the corrosive SMR atmosphere and be able to withstand thermal and pressure cycling.[4,6] We, therefore, selected in our study silicon carbide as our support material due to its superior chemical and thermal stability.[8] We deposited our PV4D4 film onto these supports via iCVD and systematically studied the conversion of the polymer into a ceramic membrane at different pyrolysis temperatures using Infrared Spectroscopy (IR) and X-ray Photoelectron Spectroscopy (XPS). To our knowledge, we are the first group to report the fabrication of a microporous ceramic membrane from the pyrolysis of polymer films deposited via iCVD.

Experimental

Support Preparation

We prepared supports by cold-pressing and sintering SiC powders into flat disks. We employed two different materials: a pure 0.6 μm β-SiC powder (Superior Graphite Co.) and a <80 nm β-SiC powder (US Research Nanomaterials). Three different supports were prepared: one

composed solely of the 0.6 μm powder, one composed solely of the <80 nm powder, and one composed of a 50/50 blend of the 0.6 μm and <80 nm powders. Prior to being pressed into a flat disk pellet, the SiC powder was mixed with boron carbide (0.1 wt.%) and phenolic resin (4 wt.%) serving as sintering aids, employing acetone as the dispersing medium. For thorough mixing of the SiC powder and the sintering aids, the resulting slurry was ultrasonicated for 20 min, then manually mixed with a spatula, and then ultrasonicated again for another 20 min. The whole procedure was repeated before the mixture was placed in a fume-hood to dry for 24 hr. The resulting material was then ground into a powder using a pestle, and oleic acid and toluene as pressing aids were then gradually added to the powder and mixed manually using a pestle and then allowed to dry for 30 min. One gr of powder was then loaded into a disk-like mold and pressed into a pellet using a hydraulic press for 2 min at a pressure of 86 MPa. The pellets were then placed in a high-temperature graphite furnace (Thermal Technology, Inc., Model 1000-3060-FP20) where they were heated (3 ºC/min) in flowing Ar to a sintering temperature of 1900 ºC, where they were kept for 3 hr., and were then cooled down (6 ºC/min) to room temperature. Prior to deposition, they were sonicated in acetone for 20 min and then dried.[37,38]

A dense iCVD layer is necessary for separation of the molecules and, therefore, an intermediate layer was first formed on the macroporous support. Without an intermediate layer, the iCVD film would uniformly coat the pores of the macroporous support instead of forming a dense layer since the pore size of the support is similar to the thickness of the iCVD layer. The intermediate layer solution was prepared by mixing 10 wt.% of allyl-hydridopolycarbosilane (AHPCS, Starfire Systems), 1.25 wt.% polystyrene (2500 MW, Sigma-Aldrich), and 5 wt.% fine SiC powder (100-200 nm) in hexane. The fine SiC powder was prepared from the original 0.6 μm SiC powder using a precipitation method described elsewhere.[39] The support was dip-coated by

immersing it in this solution for 12 sec before raising it out of the solution at a rate of 3 cm/min. The disk was then heated to 250 °C (at a rate of 3 °C/min) in flowing Ar in a tube furnace (Lindberg/Blue, Model STF55433C), where it was held for 1 hr. It was then heated to 400 °C, where it was held for another hour, and then finally heated to 750 °C, where it was held for 2 hr., before being cooled down to room temperature at a rate of 3 °C/min.

iCVD Deposition and Subsequent Pyrolysis

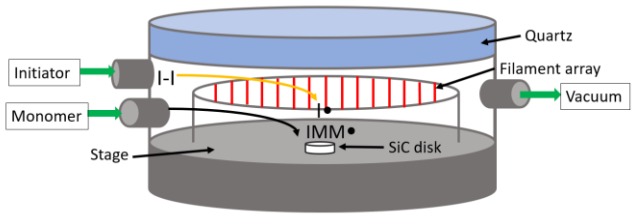

Figure 1. Schematic of the iCVD reactor

The iCVD method was used to deposit poly(2,4,6,8-tetravinyl-2,4,6,8-tetramethyl cyclotetrasiloxane) (PV4D4) onto the SiC support disks, as shown in Fig. 1. The custom-designed vacuum reactor (250 mm in diameter, 48 mm in height, GVD Corporation) has a quartz top that allows for in situ thickness measurements on a reference silicon wafer via a helium-neon laser interferometer (Industrial Fiber Optics). The support disks were placed on the reactor stage which was kept at a constant temperature of 40 °C using a recirculating chiller (Thermo Scientific Haake A25). A piece of aluminum foil was tightly wrapped and taped around the support to ensure that deposition only occurred on the top surface. A rotary-vane vacuum pump (Edwards E2M40) was used to hold the reactor under vacuum and the pressure was regulated at 190 mTorr by a throttle valve (MKS 153D) with active feedback control from a capacitance manometer (MKS 622C01TDE Baratron). The initiator and monomer liquids were loaded into stainless steel jars and introduced into the reactor through heated lines. The monomer 2,4,6,8-tetravinyl-2,4,6,8-

tetramethyl cyclotetrasiloxane (V4D4) (Gelest, Inc.) was heated to 50 °C and the flow rate was maintained at 0.7 sccm. The initiator *tert*-butyl peroxide (Aldrich, 98%) was kept at room temperature and the flow rate was maintained at 1 sccm. A nichrome filament array (Omega Engineering) was placed inside the reactor and heated to 250 °C to cleave the initiator. Approximately 1 μm of PV4D4 was deposited on each support as measured via interferometry on a reference silicon wafer.

After the deposition of the polymer, the disk was placed in a tube furnace (Lindberg/Blue, Model STF55433C) and pyrolyzed at the desired temperature over flowing argon. Prior to this pyrolysis step, flowing argon was introduced into the furnace chamber for 30 min to purge the chamber from ambient air. The sample disk was heated at a rate of 3 °C/min to 250 °C, where it was held for one hr., and then to 400 °C, where it was held for another hr., and finally to the desired pyrolysis temperature, where it was held for two more hrs., before being cooled down to room temperature at a rate of 3 °C/min.

Chemical Characterization

To determine the optimal film pyrolysis conditions, Diffuse Reflectance Infrared Fourier Transform Spectroscopy (DRIFTS) (COLLECTOR II, Thermo Scientific) was utilized. DRIFTS monitors the change in the IR spectra of a powder substrate in situ as a function of the temperature of the sample.[40] Due to SiC having a high IR radiation absorption in the mid-IR region, DX-type α-Al_2O_3 powder was chosen in this study for the DRIFTS experiments. To coat the alumina power with PV4D4, it was first spread onto a silicon wafer using a razor blade and 1 μm of PV4D4 was deposited on the alumina powder as measured on a reference wafer by interferometry. After the deposition, the PV4D4-coated powder was mixed manually with barium fluoride (BaF_2), a non-

absorbing matrix, at a ratio of 1:9 powder to BaF_2. The powder was then placed into the sample cup of the DRIFTS cell. Flowing Ar was introduced into the cell at a pressure of 69 kPa to ensure an inert atmosphere. The temperature of the DRIFTS chamber was raised in increments of 10 °C, and the IR absorbance spectra was measured every 100 °C. The DRIFTS absorbance spectra of the uncoated alumina powder was used as the background spectra.

We also measured the IR absorbance spectra of PV4D4 films ex situ by deposition onto clean silicon wafers and subsequent pyrolysis at preset temperatures. For the pyrolysis step, the PV4D4-coated wafers were placed in a tube furnace which was then purged with Ar for 30 min to ensure that no oxygen remains in the furnace. Throughout the pyrolysis process, Ar was allowed to flow through the furnace in order to ensure an inert atmosphere. The wafers were first heated to 200 °C at a rate of 2 °C/min and then kept at this temperature for 1 hr. They were then heated to 400 °C at the same rate, where they were again kept for one hr., and then finally brought up to the desired pyrolysis temperature, where the they were kept for two additional hrs. The wafers were then cooled back to room temperature at a rate of 3 °C/min. The slow heating and cooling rates are known to prevent cracking in the film.[41] After the wafers were cooled down to room temperature, the IR spectra were recorded using a FTIR spectrophotometer (Nicolet iS10, Thermo Scientific). The DRIFTS and FTIR spectra were both analyzed using the freeware SpectraGryph 1.2. and the deconvolution was performed using OriginPro Peak Analyzer.

X-ray Photoelectron Spectroscopy (XPS) analysis was used to determine the elemental composition and bonding environments of the films before and after pyrolysis at various temperatures. The Kratos Axis Ultra DLD XPS spectrometer equipped with a magnetic immersion lens and charge neutralization system and a monochromator Al X-ray source was used to collect the spectra. Survey scans were performed at a pass energy of 160 eV, while high-resolution scans

were captured at a pass energy of 40 eV. A charge correction value was applied to the C 1s environment so that the peak value was shifted to 284.8 eV. The same correction factor was applied to the Si 2p and O 1s orbitals, which resulted with the O 1s peak value being shifted to ~532 eV. Since there were signals generated from both the Si $2p_{1/2}$ and Si $2p_{3/2}$ electron spin states, it was necessary to deconvolute each silicon environment into two separate peaks. The peak area for the Si $2p_{1/2}$ was set equal to half of the peak area for the Si $2p_{3/2}$, and the full-width half-maximum (fwhm) of each spin state were set to be equal. In addition, the energy difference between the two peaks was kept constant at 0.65 eV. The number of environments we fitted per peak was based on the data obtained from our FTIR analysis. The XPS data were analyzed using the software CasaXPS. A scanning electron microscope (SEM) (Nova NanoSEM 450 Field Emission Scanning Electron Microscope) at a 15 kV accelerating voltage was also used to image the membranes.

Permeation Testing

The membranes were tested by measuring the single-gas permeance ($mol/m^2 \cdot s \cdot Pa$) of helium, hydrogen, and argon. The ideal binary separation factors were calculated by dividing the permeances of the two gasses. Prior to testing, the flat disks were glued to metal fender washer supports using an epoxy (J-B Weld) and allowed to cure for 24 hr. To measure the permeance, the metal supports were placed in between the two half-cells of the permeation system and sealed using silicone O-rings to ensure no leaks. Compressed air was used to seal the chambers via a hydraulic mechanism. The gas to be measured was introduced to the bottom half-cell at a set pressure and allowed to permeate through the membrane and to exit in the top cell. The pressure of the permeate side was kept at atmospheric condition and measured using a pressure gauge (OMEGA Engineering, DPG1000B-15G). The pressure gradient in between the top and bottom

cells was also kept constant and measured using a differential pressure transducer. The pressure on the feed side was controlled using the regulator attached to the gas cylinder and a needle valve installed on the reject-side tube. The flow rate of the permeated gas was measured with bubble-flow meters of different volumes (1 mL, 10 mL, 100 mL). The gas was allowed to fill the half-cells and permeate through the membrane for at least 30 min before data were taken to assure that steady state conditions prevail. For the permeation properties reported here, the temperature of the cell was kept at 200 °C and the transmembrane pressure difference at 241 kPa (for further details about the permeation set-up, see[38,39]).

Results and Discussion

Fig. 2a shows the iCVD polymerization of V4D4 to PV4D4. The monomer consists of a Si-O-Si cyclical structure with four vinyl bonds. Fig. 2b displays the IR spectra for both the monomer and the polymer formed via iCVD. The peaks at 960, 1400, and 1600 cm^{-1} in the monomer spectra represent the vinyl bonds. The reduction in the size of these peaks in the polymer spectra along with the increase of the symmetric stretching of CH_2 at 2920 cm^{-1} confirm that there is polymerization taking place through the vinyl bonds. In addition, there is a shift of the broad Si-O-Si bond from 1080 cm^{-1} to 1065 cm^{-1}, which is associated with the polymer.[42,43] The resulting P4V4 polymer is highly crosslinked, which has been shown to be beneficial to retain silicon groups during pyrolysis. For example, Carlsson et al.[44] found that crosslinking PDMS films, which were cast from toluene onto silicon wafers, minimized chain-scission reactions during pyrolysis which in turn prevented loss of silane groups.

To study the transition of the polymer film into a ceramic membrane at elevated temperatures, the PV4D4 film was deposited onto alumina particles and pyrolyzed in flowing Ar. The changes in the IR absorbance spectra were recorded in situ in a DRIFTS cell as its temperature

was raised up to the maximum rated temperature of the cell (~900 °C). As shown in Fig. 3, several of the distinct peaks of the PV4D4 film prior to pyrolysis were detected such as the symmetric -CH_2 stretching related to the polyethylene backbone centered at 2920 cm^{-1} (3a), the stretching of the C=C bond at 1600 cm^{-1} (3b), the wagging mode of the vinyl bond at 1415 cm^{-1} (3c), and the symmetric Si-CH_3 stretching at ~1260 cm^{-1} (3d). There was no significant change in the spectra when heating to 300 °C, indicating that the chemical structure of the polymer film stays relatively intact in this range of temperatures. There were significant changes at 400 °C such as the disappearance of the peaks corresponding to the stretching of the C=C bond and the wagging mode of the vinyl CH_2, indicating that there were no vinyl bonds left in the material. At 600 °C, there was a significant reduction in the size of the peaks corresponding to the polyethylene bonds and the symmetric Si-CH_3 bond at 1260 cm^{-1} indicating that these bonds were likely cleaved. The polyethylene peak continued to be present in small quantities until ~800 °C. The results of the DRIFTS experiments demonstrate that 600 °C is a critical temperature during which most of the hydrocarbon bonds are removed, signaling the transition to a pure silica film. Our results agree with those of Narisawa[45] who reported that the decomposition of cross-linked polysiloxane resins with methyl side groups begins first with the removal of methyl groups at ~600 °C, and the formation of silica begins beyond 1000 °C even in an oxidizing environment.

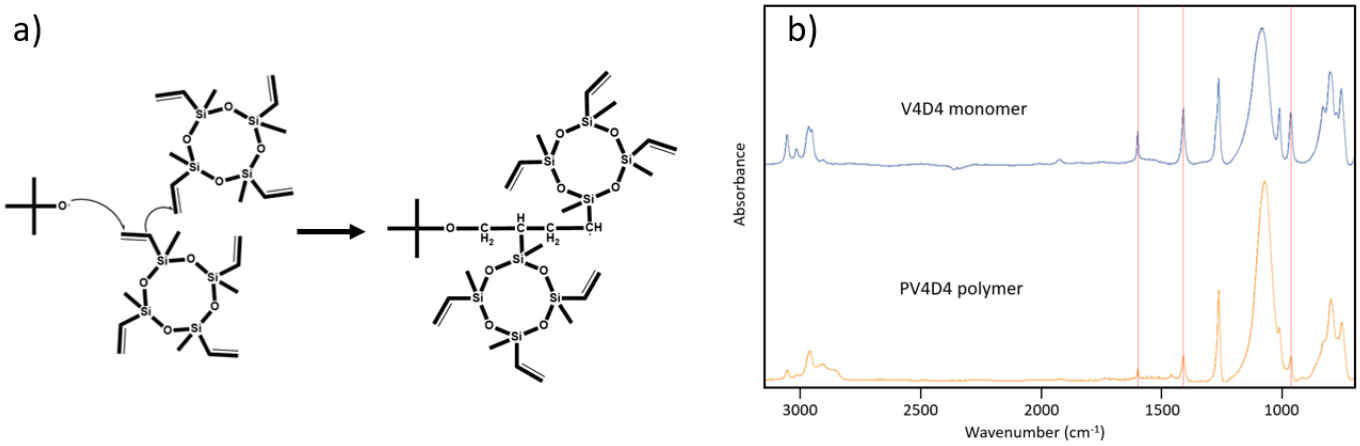

Figure 2. a) Schematic of the iCVD polymerization of V4D4 to PV4D4. b) FTIR spectra of the monomer and the resulting polymer. The dashed lines indicate the vinyl bond modes, which have a noticeable decrease in the IR spectra of the polymer.

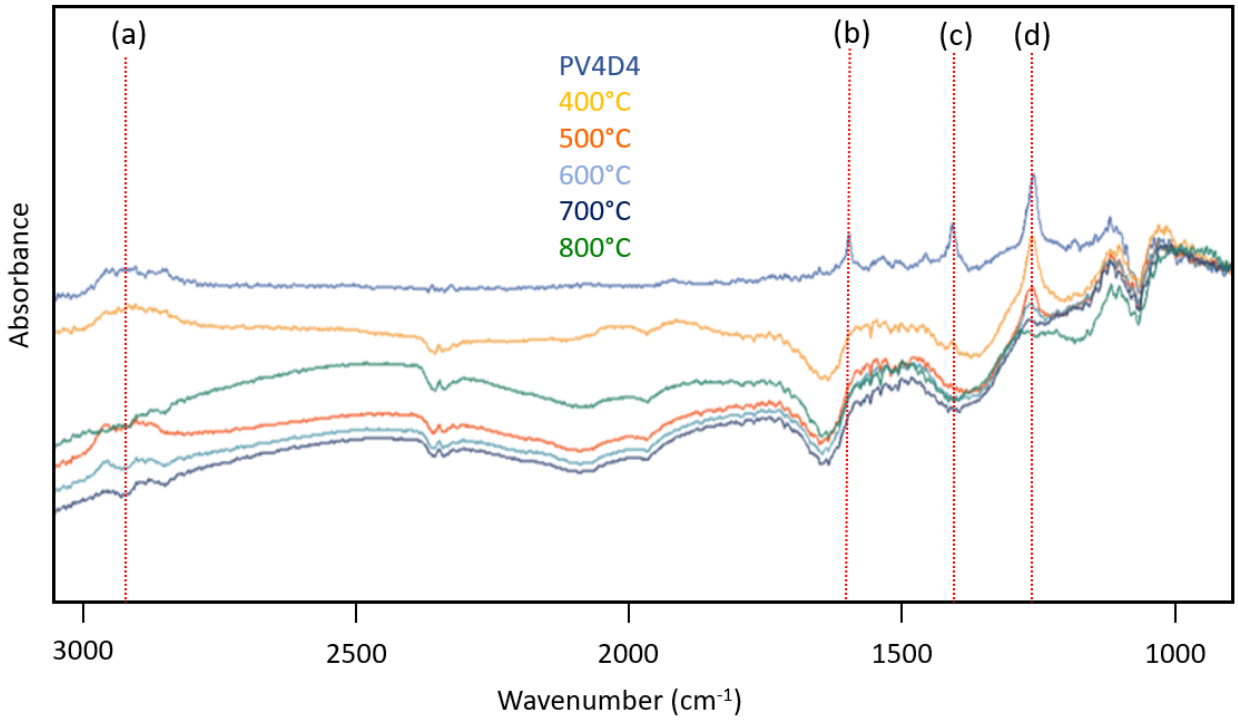

Figure 3. Real-time DRIFTS data showing the IR absorbance spectra for PV4D4 films at different pyrolysis temperatures. The dashed lines represent: a) symmetric -CH_2 stretching, b) the stretching of the C=C bond, c) the wagging mode of the vinyl bond, and d) the symmetric Si-CH_3 stretching.

Since PV4D4 does not completely convert into the ceramic until 1000 ºC and the maximum operating temperature of the DRIFTS cell is ~900 ºC, we also carried out complimentary ex situ FTIR measurements to study pyrolysis at higher temperatures. For these experiments, PV4D4 was deposited onto silicon wafers using the iCVD process, pyrolyzed in a tube furnace in flowing Ar under select pyrolysis conditions, and then the IR spectra of the resulting films were measured (Fig. 4). We monitored the change in the oxidation state of the film by monitoring the following four silicon environments: 'M' representing Si bonded to a single oxygen atom (SiO_1R_3), 'D' representing Si bonded to two oxygen atoms such as in the network polymer film (SiO_2R_2), 'T' representing Si bonded to three oxygen atoms such as in the silsesquioxane cage structure (SiO_3R), and 'Q' representing Si bonded to four oxygen atoms such as in pure silica environment (SiO_4). There is no significant change between the polymer before pyrolysis (4a) and the polymer after pyrolysis at 300 °C (4b), which is consistent with our DRIFTS experiment. For the sample pyrolyzed at 400 °C (Fig. 4c), the absorbance band at 2850-2950 cm^{-1} corresponding to the polyethylene carbon chain decreased slightly, indicating the cleavage of some of the Si-C polyethylene bonds. In addition, the bands at 960 cm^{-1}, 1415 cm^{-1}, and 1600 cm^{-1} corresponding to the vinyl bonds completely disappeared, in agreement with our results from the DRIFTS experiment. Previously, Trujillo et al.[42] studied the annealing of PV4D4 films in air up to a temperature of 410 °C, and they found that the films oxidized to form silsesquioxane-type structures. Our FTIR results show that although there are bands at 1028 cm^{-1}, corresponding to a small bond angle Si-O-Si, and at 1120 cm^{-1}, corresponding to a silsesquioxane cage ('T'), the band for the intact network at 1065 cm^{-1} ('D') still dominates the structure. This is likely because we pyrolyzed our samples under inert conditions and, therefore, there were fewer oxygen atoms readily available to allow the network rings to form the silsesquioxane cages. The Si-CH_3

stretching band shifted from 1260 cm^{-1} to a double peak at 1262 cm^{-1} and 1275 cm^{-1} and the Si-CH_3 asymmetric rocking band at 800 cm^{-1} transitioned to a double peak at 780 cm^{-1} and 800 cm^{-1}, which provides further evidence of the oxidation of some of the network groups.[42,46] For the sample pyrolyzed at 600 °C (Fig. 4d), there was an overall shift in the Si-O-Si peak from 1028 cm^{-1} to 1047 cm^{-1}. The polyethylene band centered at 2920 cm^{-1} and the bands at 1270 cm^{-1} and 2965 cm^{-1} mostly disappeared at this pyrolysis temperature. These observations are consistent with the findings of Mantz et al.[47] who reported that cylic dimethylsiloxane oligomers started decomposing at ~400 °C and that the silsesquioxane ring lost its structure in the temperature range from 450 °C - 650 ºC due to methyl abstraction. The deconvolution of the IR region between 1250 to 1270 cm^{-1} can be used to determine the ratio of M, D, and T groups in the bulk film at each pyrolysis temperature.[48,49] Figure 4b shows an expanded view of this region. It can be seen that 'D' groups dominated the deposited polymer film prior to pyrolysis. At pyrolysis temperatures of 300 °C and 400 °C, 'D' groups still dominate the structure, accounting for ~81 % and ~73 %, respectively. However, at a pyrolysis temperature of 500 °C, there was a noticeable transition to a silsesquioxane structure, with 'T' groups accounting for 48% of the structure. At a pyrolysis temperature of 600 °C, the methyl peak decreased and 'T' groups accounted for 94% of the remaining methyl bonds. Beyond 600 °C, the methyl stretching band was enveloped in the larger Si-O-Si asymmetric stretching band and it was not possible to deconvolute it. At a pyrolysis temperature of 800 °C (Fig. 4e), the Si-O-Si band continued transitioning to a silica structure with a peak shift to 1065 cm^{-1} and the silsesquioxane peak, the methyl bond, and the polyethylene absorption bands were greatly reduced.[42,45] Fig. 4f shows that pyrolysis at 1100 °C led to the formation of silica thin films as indicated by the presence of the following characteristic peaks of Si-O-Si: a rocking mode at ~450 cm^{-1}, a weak bending mode near 800 cm^{-1}, and a tall stretching vibration at ~1080 cm^{-1}.[50–52]

The shifts to these peaks, signaling the change to a pure silica 'Q' environment, were not apparent in our spectra at pyrolysis temperatures lower than 1100 °C. We also pyrolyzed PV4D4 films at 1200 °C and 1300 °C and the FTIR spectra showed no further change in the structure of the ceramic. Burns et al.[33] and Babonneau et al.[53] reported that the pyrolysis of siloxanes resins beyond 1300 °C-1500 °C resulted in the scission of Si-O bonds, with oxygen loss of up to 80% at 1600 °C. Therefore, we did not test pyrolysis at those temperatures. The consistency among the FTIR results, for which the PV4D4 film was deposited on a silicon wafer, and the DRIFTS results, for which the PV4D4 film was deposited on alumina powder, indicate that the processes that take place during the conversion of the polymer into the ceramic are substrate independent.

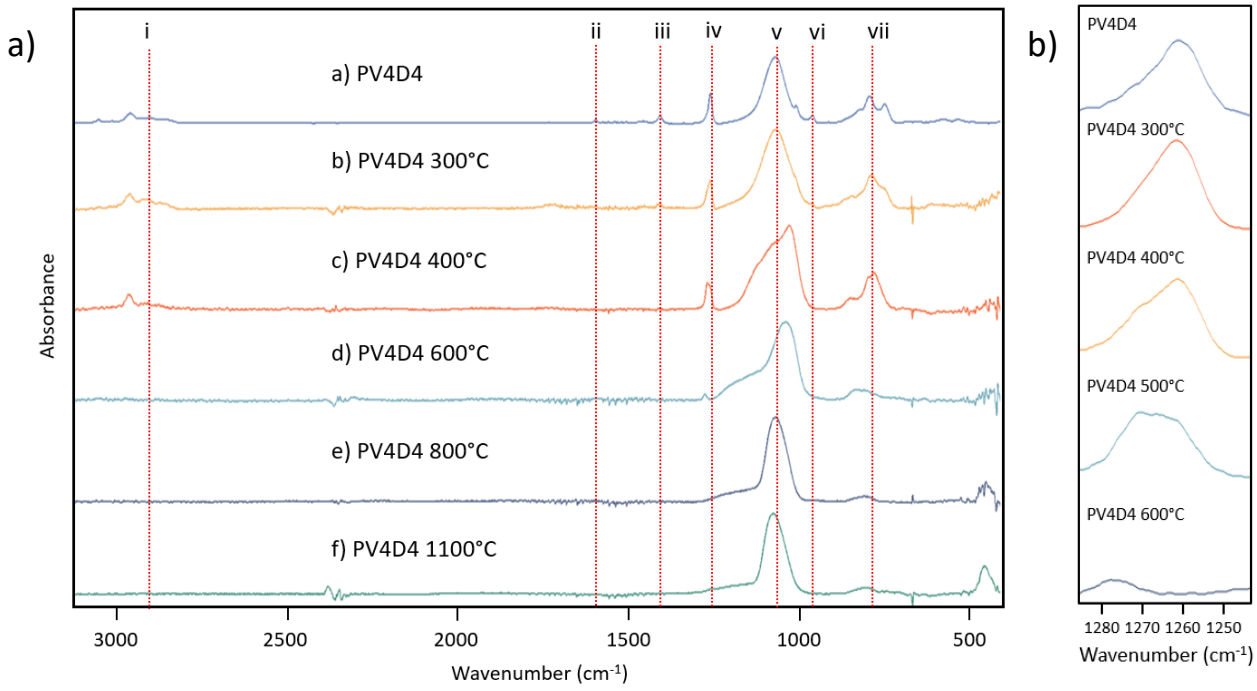

Figure 4. a) IR absorbance spectra showing the evolution of the PV4D4 film into a silica film. The absorbance bands labelled above correspond to i) the hydrocarbon bonds from the polyethylene bond, ii, iii, vi) vibration modes corresponding to vinyl bonds, iv) stretching of methyl bonds, v) asymmetric stretching of Si-O-Si bonds, and vii) asymmetric rocking in the methyl group. b) An expanded view of the IR region from 1250 to 1280 cm^{-1} showing the methyl stretching band.

Table 1. XPS elemental analysis of the PV4D4 films pre- and post-pyrolysis

Element	% Silicon	% Oxygen	% Carbon
PV4D4, theoretical	20	20	60
PV4D4, experimental	23	28	49
PV4D4, pyrolyzed at 400 °C	22	25	53
PV4D4, pyrolyzed at 600 °C	37	58	5
PV4D4, pyrolyzed at 800 °C	37	59	4
PV4D4, pyrolyzed at 1100 °C	38	60	2

The pyrolyzed PV4D4 films on silicon wafers were also analyzed by XPS to determine their chemical structure and composition. Survey scans were performed on each of the pyrolyzed films to determine the atomic fraction of carbon, oxygen, and silicon present pre- and post-pyrolysis, and the results are shown in Table 1. In agreement with the IR data, these results indicate that organic groups are removed from the PV4D4 film in increasing amounts as the temperature of pyrolysis increases. The deposited PV4D4 films had atomic compositions that were comparable to previously reported PV4D4 films deposited via iCVD.[42] There was no noteworthy shift in the elemental composition at a pyrolysis temperature of 400 °C, but there was a significant decrease in carbon content when the temperature was increased to 600 °C. This observation is consistent with the IR studies that show the disappearance of the polyethylene backbone and methyl groups, thus causing the composition of the film to shift toward the pure silica structure. At a pyrolysis temperature of 1100 °C, the silicon fraction was higher than expected from a film composed purely of 'Q' groups which would have a composition of 33.33% silicon and 66.66% oxygen.[54] The likely reason for this is the penetration of the X-ray photons through the pyrolyzed film to the underlying silicon substrate, since these films are porous due to the void space left by the organic groups that

cleave during pyrolysis. The small amount of carbon is likely indicative of surface contamination or the presence of trace amounts of carbon embedded within the structure.

In order to confirm the bonding environments in the film during the pyrolysis process, high resolution XPS scans of the silicon environment were collected. Alexander et al. [55] have shown previously that in siloxanes the oxidation state is the biggest contributing factor to the shifts in the binding energy of silicon, with reported binding energies of Si(-O_1)=101.5 eV, Si(-O_2)=102.1 eV, Si(-O_3)=102.8 eV, and Si(-O_4)=103.4 eV. O'Hare et al. [56] identified similar binding energies for these components of a siloxane film: 'M'=101.63 eV, 'D'=101.99 eV, 'T'=102.67 eV, and 'Q'=103.47 eV. The high resolution scans of the PV4D4 films pyrolyzed at different temperatures are shown in Fig. 5. The areas corresponding to each oxidation state are shown in Table 2. As was previously seen in the IR data, there was a small shift from the network structure and small bond angle Si-O-Si 'D' groups to silsesquioxane 'T' groups at a pyrolysis temperature of 400 °C. At 600 °C, there was a dramatic shift toward a mixed oxidation state, with the 'Q' groups dominating. This observation is consistent with the IR data that show that the removal of the polyethylene backbone and the methyl groups also occurs primarily between 400 °C and 600 °C. However, as with the FTIR data, there is evidence in the XPS data of residual hydrocarbon bonds, with a small number of the 'D' groups remaining. Overall, we found that there were similarities in the ratios of the silicon environments in the bulk and the surface as determined by FTIR and XPS, respectively, up to a pyrolysis temperature of 400 °C. At a pyrolysis temperature of 600 °C, 'T' groups dominated the bulk whereas 'D' groups dominated the surface. This is consistent with the observations of Corriu et al.[57], who investigated the pyrolysis of siloxane gels and found that after a pyrolysis temperature of 600 °C, 'T' siloxane materials transitioned to both 'D' and 'Q' structures due to restructuring of Si-C and Si-O bonds. Since methyl groups are cleaved and diffuse

out of the film, there is likely a higher level of recombination at the surface compared to the bulk. At ~800 °C, these groups mostly transitioned to 'Q' groups, however, residual 'D' groups were still present. The peak shifted to 103.35 eV at a pyrolysis temperature of 1100 °C, indicating the transformation of the film into silica. In summary, based on the FTIR/DRIFTS and XPS analysis results, the formation of silica film occurs at a pyrolysis temperature of 1100 °C.

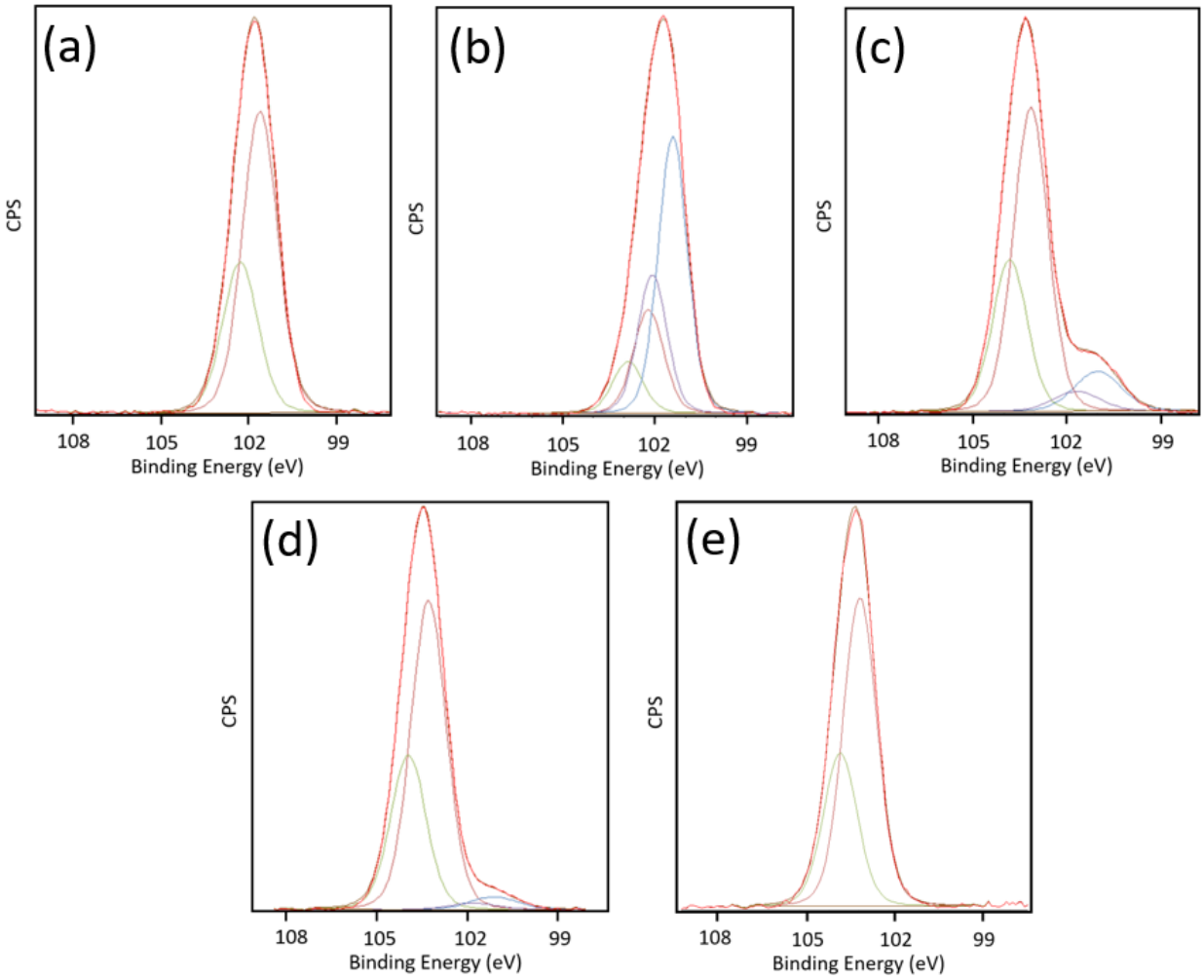

Figure 5. High resolution scans of Si 2p for the a) PV4D4 polymer and for the polymer after pyrolysis at b) 400 °C, c) 600 °C, d) 800 °C, and e) and 1100 °C.

Table 2. Peak areas of the silicon oxidation state from high resolution XPS analysis

Oxidation levels	**SiO_1**	**SiO_2**	**SiO_3**	**SiO_4**
Binding energy	-	101.8	102.6	103.4
PV4D4	0	100	0	0
400°C	0	72	28	0
600°C	0	15	0	85
800°C	0	6	0	94
1100°C	0	0	0	100

The asymmetric membranes are composed of the iCVD polymer layer deposited on SiC disks consisting of a macroporous support and an intermediate layer prepared as described in the Experimental Section. For the preparation of the membranes, the composite structure is then pyrolyzed following the procedure previously described with the final pyrolysis temperature being 1100 °C. Figure 6 shows SEM images of the resulting asymmetric structure with the polymer film deposited on the top (prior to its pyrolysis) confirming that the polymer forms a distinct layer on the surface of the SiC support disk.

Table 3 shows the permeance data for three distinct asymmetric membranes made with different supports: SiC supports composed of 50% of particles with an average diameter less than 80 nm and 50% of particles with average diameter of 0.6 μm, supports made of pure 0.6 μm SiC powders, and supports made with pure <80 nm particles. Table 3 shows the average measured permeances of He, H_2, and their ideal separation factors (defined here as the ratio of permeances) over Ar for each different type of membrane. It is important to note, that the permeances and ideal separation factors for each membrane were calculated from three distinct samples prepared under the same conditions. As can be seen in the Table, all silica films are microporous with ideal separation factors which are several times higher than the corresponding Knudsen separation factor

$\alpha_{\frac{i}{j}} = \sqrt{\frac{m_j}{m_i}}$, where m_j is the molecular weight of Ar and m_i the molecular weight of He or H_2. The mixed powder supports (0.6 μm/80 nm) resulted in an asymmetric membrane with a higher separation factor than the pure powder supports (either 0.6 μm or 80 nm). This is consistent with prior observations by our group [38], which show that utilizing larger particle sizes for supports results in bigger pores and, therefore, higher permeances and lower separation factors. However, using a mixture of powders with distinct particles sizes allows for better packing and, therefore, better separation factors with only a small sacrifice in permeance. It is important to note that there have been other silica membranes produced by both solution-phase[8,14] and conventional CVD[17,23] methods with separation factors several times larger than ours. Our future work will involve optimizing the thickness, composition, and density of the iCVD polymer film prior to its pyrolysis to improve the separation factor and permeance of the resulting membranes.

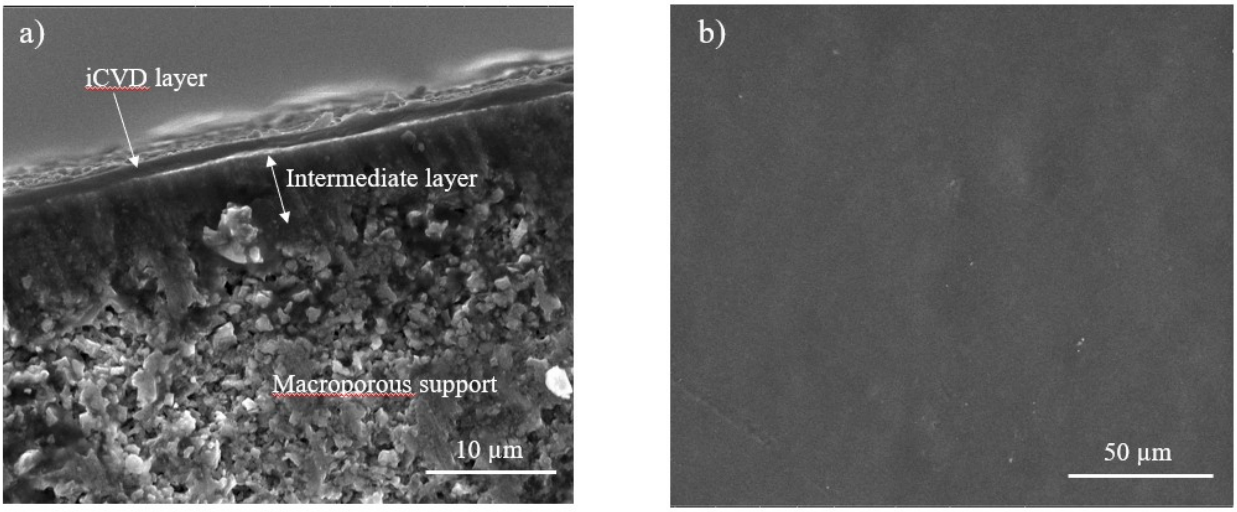

Figure 6. a) Cross-sectional view of the asymmetric composite structure consisting of the iCVD polymer layer, and the intermediate and the macroporous SiC layers, and b) top-down image of the dense iCVD layer on top of the SiC support.

Table 3. He and H_2 permeances and ideal separation factors of He and H_2 over Ar for membranes resulting from the pyrolysis at 1100 ºC of PV4D4 films deposited on SiC supports. The testing pressure was 241 kPa and the testing temperature was 473K.

Composition of the support	He permeance ($mol/m^2 \cdot Pa \cdot s$)	H_2 permeance ($mol/m^2 \cdot Pa \cdot s$)	He/Ar separation factor	H_2/Ar separation factor
100% <80 nm	4.19E-08	2.25E-08	20.7	11.0
100% 0.6μm	7.45E-07	4.81E-07	16.4	10.6
50%(<80nm)/50%(0.6μm)	2.74E-07	1.89E-07	25.1	17.4

Conclusion

In this study, we fabricated microporous silica membrane films capable of selectively separating lighter gases (e.g., H_2 and He) from bulkier gases (e.g., Ar) through the deposition and subsequent pyrolysis of PV4D4 films. We used in situ DRIFTS and complimentary ex situ FTIR studies to investigate the chemical structure of PV4D4 at different pyrolysis temperatures and found that the network and silsesquioxane-dominated bonding environment shifted to a largely silica 'Q' bonding environment at 600 °C. It was not until the pyrolysis temperature reached 1100 °C, however, that we saw a complete transformation into a silica structure. In addition to the DRIFTS/FTIR studies, we also used XPS to analyze the films after pyrolysis. The XPS results confirm that organic groups were removed from the film structure as the temperature of pyrolysis increased. The high resolution XPS analysis allowed us to identify the oxidation state of each film and to establish that 1100 °C was the pyrolysis temperature at which a pure silica film was formed. Therefore, we used this pyrolysis temperature to prepare silica membrane films on SiC support disks to measure their permeation properties. The resulting membrane films were shown to be microporous and capable of separating light gases. The nature of the supports also has an influence

on the properties of the resulting membrane films with mixed-powder supports exhibiting higher separation factors.

Acknowledgements

The authors acknowledge the support of the ACS Petroleum Research Fund (PRF) and the National Science Foundation (Award# CBET-1705180). XPS data and SEM images were acquired at the Core Center of Excellence in Nano Imaging at the University of Southern California.

References:

(1) Song, C.; Liu, Q.; Ji, N.; Kansha, Y.; Tsutsumi, A. Optimization of Steam Methane Reforming Coupled with Pressure Swing Adsorption Hydrogen Production Process by Heat Integration. *Appl. Energy* **2015**, *154*, 392–401.

(2) da Silva Veras, T.; Mozer, T. S.; da Costa Rubim Messeder dos Santos, D.; da Silva César, A. Hydrogen: Trends, Production and Characterization of the Main Process Worldwide. *Int. J. Hydrogen Energy* **2017**, *42* (4), 2018–2033.

(3) Tsuru, T.; Morita, T.; Shintani, H.; Yoshioka, T.; Asaeda, M. Membrane Reactor Performance of Steam Reforming of Methane Using Hydrogen-Permselective Catalytic SiO2membranes. *J. Memb. Sci.* **2008**, *316* (1–2), 53–62.

(4) Ockwig, N. W.; Nenoff, T. M. Membranes for Hydrogen Separation. In *Chemical Reviews*; 2007; pp 4078–4110.

(5) Beurden, P. va. On The Catalytic Aspects Of Steam Reforming Methane - A Literature Survey. *ECN* **2004**, 1–27.

(6) Gallucci, F.; Comite, A.; Capannelli, G.; Basile, A. Steam Reforming of Methane in a Membrane Reactor: An Industrial Case Study. *Ind. Eng. Chem. Res.* **2006**, *45* (9), 2994–3000.

(7) Baker, R. W. *Membrane Technology and Applications*, Third.; John Wiley & Sons: West Sussex, 2012.

(8) Elyassi, B. Inorganic Membranes. *Encyclopedia of Chemical Processing*; 2009; pp 1–16.

(9) Gallucci, F.; Fernandez, E.; Corengia, P.; van Sint Annaland, M. Recent Advances on Membranes and Membrane Reactors for Hydrogen Production. *Chem. Eng. Sci.* **2013**, *92*, 40–66.

(10) Uemiya, S. Brief Review of Steam Reforming Using a Metal Membrane Reactor. *Top. Catal.* **2004**, *29* (1/2), 79–84.

(11) Fernandes, F. A. N.; Soares, A. B. Modeling of Methane Steam Reforming in a Palladium Membrane Reactor. *Lat. Am. Appl. Res.* **2006**, *36* (3), 155–161.

(12) Xu, X.; Yang, W.; Song, C.; Liu, J.; Lin, L. Hydrogen Separation by Zeolite Membranes. *ACS Div. Fuel Chem. Prepr.* **2003**, *48* (1), 284–285.

(13) Parsley, D.; Ciora, R. J.; Flowers, D. L.; Laukaitaus, J.; Chen, A.; Liu, P. K. T.; Yu, J.; Sahimi, M.; Bonsu, A.; Tsotsis, T. T. Field Evaluation of Carbon Molecular Sieve Membranes for the Separation and Puri Fi Cation of Hydrogen from Coal- and Biomass-Derived Syngas. *J. Memb. Sci.* **2014**, *450*, 81–92.

(14) Lin, Y. S.; Kumakiri, I.; Nair, B. N.; Alsyouri, H. Microporous Inorganic Membranes. *Sep. Purif. Methods* **2002**, *31* (2), 229–379.

(15) Shelekhin, A. B.; Dixon, A. G.; Ma, Y. H. Theory of Gas Diffusion and Permeation in Inorganic Molecular Sieve Membranes. *AIChE J.* **1995**, *41* (1), 58–67.

(16) Jimenez, G.; Dillon, E.; Dahlmeyer, J.; Garrison, T.; Garrison, T.; Darkey, S.; Wald, K.; Kubik, J.; Paciulli, D.; Talukder, M.; et al. A Comparative Assessment of Hydrogen Embrittlement : Palladium and Silver) Subjected to Hydrogen Absorption / Desorption Cycling. *Adv. Chem. Eng. Sci.* **2016**, *6* (July), 246–261.

(17) Sheima Jatib Khatib, S. Ted Oyama, Katia R. de Souza, A.; Noronha, F. B. Review of Silica Membranes for Hydrogen Separation Prepared by Chemical Vapor Deposition. In *Membrane Science and Technology*; 2011; pp 25–60.

(18) Satvekar, R.; Society, D. Y. P. E.; Phadatare, M. R.; Society, D. Y. P. E.; Tiwale, B. M.; Pawar, S. H. Influence of Silane Content on the Optical Properties of Sol Gel Derived Spin Coated Silica Thin Films. *Int. J. Basic Appl. Sci.* **2012**, *4* (October 2014), 468–476.

(19) Saputra, R. E.; Astuti, Y.; Darmawan, A. Spectrochimica Acta Part A : Molecular and Biomolecular Spectroscopy Hydrophobicity of Silica Thin Films : The Deconvolution and Interpretation by Fourier-Transform Infrared Spectroscopy. *Spectrochim. Acta Part A Mol. Biomol. Spectrosc.* **2018**, *199*, 12–20.

(20) Khalib, N. A. Z. Fabrication of Silica Ceramic Membrane via Sol-Gel Dip-Coating Method at Different Nitric Acid Amount Fabrication of Silica Ceramic Membrane via Sol-Gel Dip-Coating Method at Different Nitric Acid Amount. *IOP Conf. Ser. Mater. Sci. Eng.* **2018**, *290*.

(21) Boffa, V.; Blank, D. H. A.; Elshof, J. E. Hydrothermal Stability of Microporous Silica and Niobia – Silica Membranes. *J. Memb. Sci.* **2008**, *319* (1–2), 256–263.

(22) Seidel, S.; Riche, C.; Gupta, M. Chemical Vapor Deposition of Polymer Films. *Encycl. Polym. Sci. Technol.* **2011**.

(23) Iarikov, D. D.; Hacarlioglu, P.; Oyama, S. T. *Amorphous Silica Membranes for H 2 Separation Prepared by Chemical Vapor Deposition on Hollow Fiber Supports*, 1st ed.; Elsevier B.V., 2011; Vol. 14.

(24) Sheima J. Khatib, S. T. O. Silica Membranes for Hydrogen Separation Prepared by Chemical Vapor Deposition (CVD). *Sep. Purif. Technol.* **2013**, *111*, 20–42.

(25) Nagasawa, H.; Minamizawa, T.; Kanezashi, M.; Yoshioka, T.; Tsuru, T. High-Temperature Stability of PECVD-Derived Organosilica Membranes Deposited on TiO 2

and SiO 2 – ZrO 2 Intermediate Layers Using HMDSO / Ar Plasma. *Sep. Purif. Technol.* **2014**, *121*, 13–19.

(26) Nagasawa, H.; Minamizawa, T.; Kanezashi, M.; Yoshioka, T. Microporous Organosilica Membranes for Gas Separation Prepared via PECVD Using Different O / Si Ratio Precursors. *J. Memb. Sci.* **2015**, *489*, 11–19.

(27) Baxamusa, S. H.; Im, S. G.; Gleason, K. K. Initiated and Oxidative Chemical Vapor Deposition: A Scalable Method for Conformal and Functional Polymer Films on Real Substrates. *Phys. Chem. Chem. Phys.* **2009**, *11* (26), 5227–5240.

(28) Gupta, M.; Gleason, K. K. Initiated Chemical Vapor Deposition of Poly(1H,1H,2H,2H-Perfluorodecyl Acrylate) Thin Films. *Langmuir* **2006**, *22* (24), 10047–10052.

(29) Cheng, C.; Gupta, M. Surface Functionalization of 3D-Printed Plastics via Initiated Chemical Vapor Deposition. *Beilstein J. Nanotechnol.* **2017**, *8* (1), 1629–1636.

(30) Haller, P. D.; Flowers, C. A.; Gupta, M. Three-Dimensional Patterning of Porous Materials Using Vapor Phase Polymerization. *Soft Matter* **2011**, *7*, 2428–2432.

(31) Cheng, C.; Gupta, M. Roll-to-Roll Surface Modification of Cellulose Paper via Initiated Chemical Vapor Deposition. *Ind. Eng. Chem. Res.* **2018**, *57* (34), 11675–11680.

(32) Wilson, A. M.; Zank, G.; Eguchi, K.; Xing, W.; Yates, B.; Dahn, J. R. Polysiloxane Pyrolysis. *Chem. Mater.* **1997**, *9* (7), 1601–1606.

(33) Burns, G. T.; Taylor, R. B.; Xu, Y.; Zangvil, A.; Zank, G. A. High-Temperature Chemistry of the Conversion of Siloxanes to Silicon Carbide. *Chem. Mater.* **1992**, *4* (6), 1313–1323.

(34) Naserifar, S.; Goddard, W. A.; Liu, L.; Tsotsis, T. T.; Sahimi, M. Toward a Process-Based Molecular Model of SiC Membranes. 2. Reactive Dynamics Simulation of the Pyrolysis of Polymer Precursor to Form Amorphous SiC. *J. Phys. Chem. C* **2013**, *117* (7), 3320–3329.

(35) Gao, H.; Wang, H.; Zhao, Z.; Niu, M.; Su, L.; Wei, Y. Reactive Dynamics Simulation Study on the Pyrolysis of Polymer Precursors to Generate Amorphous Silicon Oxycarbide Structures. *J. Phys. Chem. C* **2018**, *122* (10), 5767–5773.

(36) Sarkar, S.; Gan, Z.; An, L.; Zhai, L. Structural Evolution of Polymer-Derived Amorphous SiBCN Ceramics at High Temperature. *J. Phys. Chem. C* **2011**, *115* (50), 24993–25000.

(37) Elyassi, B.; Deng, W.; Sahimi, M.; Tsotsis, T. T. On the Use of Porous and Nonporous Fillers in the Fabrication of Silicon Carbide Membranes. *Ind. Eng. Chem. Res.* **2013**, *52* (30), 10269–10275.

(38) Deng, W.; Yu, X.; Sahimi, M.; Tsotsis, T. T. Highly Permeable Porous Silicon Carbide Support Tubes for the Preparation of Nanoporous Inorganic Membranes. *J. Memb. Sci.* **2014**, *451*, 192–204.

(39) Dabir, S.; Deng, W.; Sahimi, M.; Tsotsis, T. Fabrication of Silicon Carbide Membranes on Highly Permeable Supports. *J. Memb. Sci.* **2017**, *537*, 239–247.

(40) ThermoSpectraTech. *COLLECTOR ™ II User ' s Manual*.

(41) Raj, R.; Pederiva, L.; Narisawal, M.; Soraru, G. D. On the Onset of Fracture as a Silicon-Based Polymer Converts into the Ceramic Phase. *J. Am. Ceram. Soc.* **2018**, *102* (3), 924–929.

(42) Trujillo, N. J.; Wu, Q.; Gleason, K. K. Ultralow Dielectric Constant Tetravinyltetramethylcyclotetrasiloxane Films Deposited by Initiated Chemical Vapor Deposition (ICVD). *Adv. Funct. Mater.* **2010**, *20* (4), 607–616.

(43) J. Lubguban, T. Rajagopalan, N. Mehta, B. Lahlouh, S. L. Simon, and S. G. Low- k Organosilicate Films Prepared by Tetravinyltetramethylcyclotetrasiloxane. *Appl. Phys.* **2002**, *92* (2), 1033–1038.

(44) Carlsson, D. J.; Cooney, J. D.; Gauthier, S.; Worsfold, D. J. Pyrolysis of Silicon-Backbone Polymers to Silicon Carbide. *Am. Ceram. Soc.* **1990**, *73* (2), 237–241.

(45) Narisawa, M. Silicone Resin Applications for Ceramic Precursors and Composites. *Materials (Basel).* **2010**, *3* (6), 3518–3536.

(46) Ryan, E. T.; Gates, S. M.; Cohen, S. A.; Ostrovski, Y.; Adams, E.; Virwani, K.; Virwani, K.; Grill, A. Effect of Low-Frequency Radio Frequency on Plasma-Enhanced Chemical Vapor Deposited Ultra Low- κ Dielectric Films for Very Large- Scale Integrated Interconnects Interconnects. *Appl. Phys.* **2014**, *115* (144107).

(47) Mantz, R. A.; Jones, P. F.; Chaffee, K. P.; Lichtenhan, J. D.; Gilman, J. W. Thermolysis of Polyhedral Oligomeric Silsesquioxane (POSS) Macromers and POSS - Siloxane Copolymers. *Chem. Mater.* **1996**, *8* (6), 1250–1259.

(48) Burkey, D. D.; Gleason, K. K. Temperature-Resolved Fourier Transform Infrared Study of Condensation Reactions and Porogen Decomposition in Hybrid Organosilicon-Porogen Films Temperature-Resolved Fourier Transform Infrared Study of Condensation Reactions and Porogen Decomposition in Hy. *J. Vac. Sci. Technol.* **2003**, *22* (1), 61–70.

(49) Burkey, D. D.; Gleason, K. K. Structure and Mechanical Properties of Thin Films Deposited from 1,3,5-Trimethyl-1,3,5- Trivinylcyclotrisiloxane and Water. *J. Appl. Phys.* **2003**, *93* (9), 5143–5150.

(50) Samitier, J.; Marco, S.; Morante, J. R. Analysis by FT-IR Spectroscopy of SiO , - Polycrystalline in Micromechanics : Stress Measurements. *Sensors and Actuators* **1992**, *32*, 347–353.

(51) Haleh Sanaeishoar, Maryam Sabbaghan, F. M. Synthesis and Characterization of Micro-Mesoporous MCM-41 Using Various Ionic Liquids as Co-Templates. *Microporous Mesoporous Mater.* **2015**, *217*, 219–224.

(52) Shokri, B.; Firouzjah, M. A.; Hosseini, S. I. FTIR Analysis of Silicon Dioxide Thin Film Deposited by Metal Organic-Based. In *19th international symposium on plasma chemistry society, Bochum, Germany*; 2009; pp 1–4.

(53) Babonneau, F.; Thorne, K.; Mackenzie, J. D. Dimethyldiethoxysilane/Tetraethoxysilane Copolymers: Precursors for the Silicon-Carbon-Oxygen System. *Chem. Mater.* **2005**, *1* (5), 554–558.

(54) Mabboux, P.; Gleason, K. K. Chemical Bonding Structure of Low Dielectric Constant Si : O : C : H Films Characterized by Solid-State NMR. *J. Electrochem. Soc.* **2005**, *152* (1), F7–F13.

(55) Alexander, M. R.; Short, R. D.; Jones, F. R. A Study of HMDSO/O2 Plasma Deposits Using a High-Sensitivity and -Energy Resolution XPS Instrument : Curve Fitting of the Si 2p Core Level. *Appl. Surf. Sci.* **1999**, *137* (1–4), 179–183.

(56) Hare, L. O.; Parbhoo, B.; Leadley, S. R. Development of a Methodology for XPS Curve-Fitting of the Si 2p Core Level of Siloxane Materials. *Surf. Interface Anal.* **2004**, *36* (10), 1427–1434.

(57) Belot, V.; Corriu, R.; Leclercq, D.; Mutin, P. H.; Vioux, A. Thermal Reactivity of Hydrogenosilsesquioxane Gels. *Chem. Mater.* **1991**, *3* (1), 127–131.

For Table of Contents use only: